International Journal of Concrete Structures and Materials

RESEARCH

Open Access

Experimental Investigation of the Eccentric Performance of Columns Reinforced by Steel and GFRP Bars and Strengthened with GFRP NSM Bars and Mat Techniques

Seleem S. E. Ahmad[1*], Mohamed Yones[1], Mahmoud Zaghlal[2], Hesham Elemam[1,3] and Ahmed A. Elakhras[1]

Abstract

An experimental program was conducted to study the eccentric behavior of columns reinforced with glass fiber-reinforced polymer (GFRP), steel bars, or a hybrid of both. Two strengthening methods were employed: GFRP mats and near surface-mounted (NSM) GFRP bars. Eighteen specimens with different reinforcement configurations, all having slenderness ratios 19, were tested under axial compression loads with eccentricities of 0.0 mm, 30 mm, and 60 mm. Results showed that using GFRP bars as longitudinal reinforcement significantly decreased the axial bearing capacity as eccentricity increased, with reductions of about 43% at 30 mm and 71% at 60 mm without additional strengthening. Specimens strengthened with three layers of GFRP mats exhibited reductions of approximately 35% and 56% at the same eccentricities, while a combination of GFRP mats and NSM bars showed reductions of 19% and 49%. At zero eccentricity, NSM GFRP rebars combined with GFRP wrap increased the loading capacity by about 10% and enhanced ductility by approximately 54%. Combining NSM GFRP rebars and GFRP wrap can significantly increase the loading capacity and improve displacement ductility. The obtained results show that these specimens outperform others. For example, the axial load is increased by 10% at $e=0$, by 56% at $e=30$, and by 93% at $e=60$ compared to the control specimens. The elastic stiffness was comparable for columns reinforced with GFRP and steel. Using GFRP for longitudinal reinforcement and steel for stirrups resulted in a 16% reduction in axial load and a 22% reduction in axial displacement. The strengthening techniques proved more effective as the loading eccentricity approached the P–M curve's equilibrium point.

Highlights

- Eccentricity diminishes the columns' axial bearing capacity.
- Hybrid reinforcement for columns affects load-bearing capacity and ductility.
- Strengthening by NSM GFRP bars and GFRP wrap increases loading capacity.
- Strengthening was effective as the load eccentricity increased to the P–M curves' balance.

Journal information: ISSN 1976-0485 / eISSN 2234-1315.

*Correspondence:
Seleem S. E. Ahmad
ssdawod@eng.zu.edu.eg
Full list of author information is available at the end of the article

Keywords Hybrid reinforcement, GFRP bars, GFRP mat, Eccentricity, NSM, Axial compression, Confinement, Bending moment

1 Introduction

GFRP, or glass fiber-reinforced polymer, is popular for strengthening structures due to its strength, durability, and corrosion resistance. However, GFRP is vulnerable to breakage due to its low elasticity modulus, especially in columns. Previous studies have extensively employed GFRP in various applications when comparing the elastic moduli of steel (El-Emam et al., 2020a, 2020b, 2024). Rectangular column specimens with varying slenderness ratios, reinforcement ratios, loading conditions (centric and eccentric), and different stirrup spacing were utilized (Elchalakani & Ma, 2017; Khorramian & Sadeghian, 2020; Sun et al., 2017). The results indicated that GFRP bars could sustain compressive loads even after the concrete had been crushed, attributed to the contribution of GFRP in compression. Additionally, the load–deflection capacity of columns increased with decreasing stirrup spacing. However, the force–deformation curves did not align with those of steel-reinforced columns before reaching the ultimate load. The circular columns were studied with different slenderness ratios, reinforcement ratios, diameters, and spacing between the spiral stirrups. The effect of high-strength concrete (HSC) with GFRP reinforcement was also investigated (Abdelazim et al., 2020; Afifi et al., 2014; Hadhood et al., 2017; Mohamed et al., 2014). Tests were conducted under concentric and eccentric loads with varying eccentric distances from the axis, and the results were compared with samples cast using steel reinforcement. The test results showed the efficiency of GFRP bars compared to steel reinforcement in the non-central samples, where compressive failure dominated with slight deflection. In samples with significant eccentric loading, bending failure in tension predominated. Additionally, reducing the diameter and spacing between the spiral stirrups increases the load-bearing capacity of the column. The work (Fillmore & Sadeghian, 2018) confirmed that GFRP can withstand high levels of compression for an extended period after reaching the maximum load without premature crushing. It also concluded that although the modulus of elasticity in tension is higher than that in compression for GFRP, the compressive strength was obtained at 67% of the tensile strength.

The effect of reinforcement ratio, the number of longitudinal bars, and the spacing between spiral stirrups were studied for high-strength hollow columns (AlAjarmeh et al., 2019, 2020). The two studies demonstrated that a higher resistance can be achieved at the same reinforcement ratio by increasing the number of bars while reducing their diameter or by decreasing the spacing between the spiral stirrups. Upon examining the studies that used GFRP, it is evident that the failure in the columns does not occur in the concrete cover; when the columns reach their maximum load, the failure begins to propagate inward, including the GFRP. This issue leads to a brittle failure of the columns.

Previous works have provided methods for strengthening various columns regarding shape, slenderness ratio, concrete type, and internal reinforcement ratio. Rectangular columns were strengthened by wrapping them with GFRP fabric, and the results showed a significant increase in the axial load capacity of the column when wrapped with GFRP fabrics. Wrapping the column completely using strips was more effective than using continuous fabric. As the number of wrap layers increased, the column's load-bearing capacity also increased, along with improved ductility. Moreover, the results indicated that using GFRP enhances strength, which is significantly influenced by the aspect ratio of the cross-section (Kumutha et al., 2007; Sai Madupu & Sai Ram, 2021; Sudhakar & Partheeban, 2017). The methods for strengthening circular, square, and rectangular columns were studied (Raval & Dave, 2013), and the results showed that the stress–strain behaviors indicated that the strength gained from FRP confinement was prominent in circular columns, while the increase in strength for square and rectangular columns was less, due to the variation in lateral confining pressure distribution. The methods for strengthening square-shaped columns with light internal reinforcement were studied (Triantafyllou et al., 2015). The strength and ductility levels achieved in the strengthened columns indicate that partial wrapping can effectively enhance the mechanical behavior of square cross-section columns.

The behavior of a strengthening system consisting of pre-manufactured carbon fiber-reinforced polymer (CFRP) laminates and glass fiber-reinforced polymer (GFRP) wraps was studied (Khorramian & Sadeghian, 2021). The test results showed that using wraps without longitudinal CFRP laminates was more effective than the proposed hybrid system for strengthening small-scale concrete columns subjected to pure axial loading. For slender columns, the hybrid system enhanced the wrapping system with increases in axial capacity, flexural

capacity, and lateral displacement at peak load, respectively, by altering the load–deflection curve of the slender columns to achieve a higher performance level. The squared samples were used to study the reduction of non-uniform distribution in square columns by examining the number of GFRP layers and the corner radius of the square shape (Benzaid et al., 2008). The results indicated that a larger radius could expand the strong constraint zone and reduce stress concentration. Thus, the reduced confining pressure in the square section due to stress concentration at the corners is addressed using a square section with rounded corners.

The strengthening of columns using a hybrid system consisting of near-surface mounted (NSM) reinforcement and externally bonded (EB) GFRP or CFRP wraps was investigated (Chellapandian et al., 2019; Esfandi Sarafraz, 2019; Talaeitaba et al., 2019). The results demonstrated an improvement in stiffness and strength under compressive loads. This enhancement was attributed to the contribution of NSM reinforcement to flexural resistance. Moreover, the study (Gajdošová & Bilčík, 2013) demonstrates that carbon fiber reinforcement effectively strengthens slender columns. The results indicate that strips used in the NSMR method significantly improve the behavior of slender columns, while CFRP sheets enhance the performance of short columns.

The effectiveness of strengthening systems in concrete columns, including those subjected to moments, has been demonstrated (Neupane, et al., 2024). This study investigates the effectiveness of post-tensioned metal straps (PTMS) in enhancing the performance of low-strength reinforced concrete (LS RC) columns. The results indicate that PTMS confinement significantly improved the columns' load-carrying capacity and deformation resistance. The study concludes that PTMS confinement is a promising technique for strengthening LS RC columns.

Experimental and numerical studies examined the behavior of exterior reinforced concrete (RC) beam–column joints repaired and strengthened with post-tensioned metal straps (PTMS) for active confinement, as detailed in reference (Helal et al., 2024). The results showed that the ASCE/SEI 41–17 guidelines accurately predict the shear capacity of bare joints. Recasting the core with new concrete increased shear capacity by up to 42%, while further strengthening with PTMS enhanced it by 25%.

The effectiveness of strengthening low-strength reinforced concrete (RC) beams with near-surface mounted (NSM) carbon fiber-reinforced polymer (CFRP) rods was examined in Imjai et al. (2022). The results show that this method increases the cracking load of the beams by up to 19%. Additionally, the yield and ultimate load capacities rise by up to 31% and 64%, respectively. The moment–curvature and finite element (FE) methods accurately predict deflections of the strengthened RC beams within 20% and 10% at failure (El-Sisi et al., 2022; Sallam et al., 2013).

Previous studies examined various strengthening methods for reinforced concrete columns with steel. For example, the columns were externally wrapped using GFRP (Glass Fiber Reinforced Polymer) or CFRP (Carbon Fiber Reinforced Polymer). These studies investigated various factors, including the number of layers used for wrapping the column, the column cross-section, and the slenderness ratio of the columns. Additionally, a hybrid strengthening system was utilized, which combined near surface mounted (NSM) reinforcement with the wrapping system.

The studies showed that the hybrid system significantly improved results, as the longitudinal reinforcement contributes to bearing internal stresses while the wraps enhance confinement. This combination allows the NSM system to handle greater loads without failure than the column alone.

2 Research Significance

This study provides critical insights into the structural behavior of columns reinforced with Glass Fiber-Reinforced Polymer (GFRP), steel, or a hybrid of both under varying eccentric loading conditions. The research addresses a gap in the literature by evaluating the performance of locally manufactured GFRP reinforcement and its potential to replace or complement traditional steel reinforcement. By employing two strengthening techniques, GFRP mats and near surface-mounted (NSM) GFRP rebars, this study investigates their effectiveness in improving load-carrying capacity, ductility, and stiffness across different eccentricities.

3 Experimental Investigation

3.1 Experimental Outline

The experimental program outline consisted of 18 specimens measuring 850 mm long and a rectangular cross-section of 150×150 mm. The slenderness ratio ($\lambda = kl/r \leq 22$) is for short columns, as known from the Egyptian code for the design of reinforced concrete structures ECP 203–2007. The dimensions of the specimens in the present work were chosen to give $\lambda \leq 22$ ($\lambda = 19$), and thus, the buckling effects may be considered very small and can be neglected. This assumption can be found in other works (Abdelazim et al., 2020; Khorramian & Sadeghian, 2020, 2021). The configurations of the specimens are detailed in Table 1. Twelve specimens were divided into groups based on specific variables under investigation, undergoing centric and eccentric loading tests. Of

Table 1 Configurations of the tested specimens

Specimen ID	Main reinforcement	Ties type	Mat confinement	Eccentricity (e), mm	NSM
Ss-0lay-0-0	Steel	Steel	Without	0	Non
Ss-0lay-0-30				30	
Sg-0lay-0-0		GFRP		0	
Sg-0lay-0-30				30	
Gs-0lay-0-0 Sg-0lay-N-*e*="30"	GFRP	Steel		0	
Gs-0lay-0-30				30	
Gg-0lay-0-0		GFRP		0	
Gg-0lay-0-30				30	
Gg-0lay-0-60				60	
Gg-1lay-0-0			1 layer of GFRP wrapping	0	
Gg-1lay-0-30				30	
Gg-1lay-0-60				60	
Gg-3lay-0-0			3 layers of GFRP wrapping	0	
Gg-3lay-0-30				30	
Gg-3lay-0-0				60	
Gg-3lay-N-0				0	8 bars
Gg-3lay-N-30				30	
Gg-3lay-N-60				60	

these, three specimens served as non-wrapped controls, while three were wrapped with a single layer of GFRP, another three with three layers of GFRP, and the remaining three with three layers of GFRP along with eight-bar GFRP near surface mounted (NSM).

The second group, consisting of six members, underwent additional strengthening methods: two specimens featured stirrups and primary reinforcement with steel bars, two with stirrups and main reinforcement using GFRP bars, and the final two with both stirrups and primary reinforcement reinforced with GFRP bars. The specimens were subjected to axial compression loads at 0-, 30-, and 60-mm eccentricities during testing.

As shown in Table 1, the general format for the specimen ID is (Aa-blay-c-e). In this format, the letter (A) denotes the type of longitudinal reinforcing bar, with 'S' indicating steel and 'G' indicating GFRP. The letter (a) specifies the type of stirrup: 's' for steel stirrups and 'g' for GFRP stirrups. The letter (b) represents the number of GFRP wrap layers, while (c) indicates the NSM (near-surface-mounted): '0' for without NSM and 'N' for with NSM. Lastly, the letter (e) denotes the eccentric distance, which can be 0, 30, or 60 mm. For example, a specimen ID of (Gg-3lay-0-30) signifies a specimen featuring GFRP longitudinal bars and stirrups, wrapped with three layers of GFRP wraps, 0 is no NSM are used, and subjected to an eccentric load of 30 mm.

3.2 Material Properties

Locally available siliceous sand with a specific gravity of 2.6 and a fineness modulus of 2.39 served as the fine aggregate. Coarse aggregate consisted of dolomite with a specific gravity of 2.65, a water absorption rate of 0.90%, and a nominal maximum size of 12 mm. Suez Cement's Type I Ordinary Portland Cement, Grade 42.5N, was chosen for the mix. A superplasticizer was added at a rate of 8 l per cubic meter, and the water-to-cement ratio was maintained at 0.33. Specific proportions of the concrete mix are detailed in Table 2. Concrete cubes measuring $150\times150\times150$ mm were subjected to compressive strength testing to evaluate the material properties, yielding an average value of 50 MPa. Steel reinforcement was employed with a tensile strength of 400 MPa and a yield strength of 360 MPa. The NSM and GFRP reinforcement utilized had a modulus of elasticity of 50 GPa and a tensile strength of 1000 MPa. Stirrups made of GFRP

Table 2 The mix proportions for cubic meters of concrete

Material	Cement, kg	W/C	Sand, kg	Dolomite, kg	Water, lit	Superplasticizer, kg
Amount	500	0.33	750	1000	166.75	8

rebar exhibited a yield strength of 617 MPa and a tensile strength of 730 MPa. Juni strengthening two-way wraps (444 g/m^2) were selected for connecting FRP bars with concrete, along with Kemapoxy 165 epoxy resin from CMB. Boytek BRE 452 polyester resin was chosen for adhesive wraps. The material parameters provided by the manufacturer are given in Table 3.

Table 3 Mechanical properties of the used GFRP wrap, epoxy, and polyester

No	Material type	Ultimate tensile strength (MPa)	Modulus of elasticity (GPa)
1	GFRP wrap	2500-2700	81–84
2	(Boytek BRE 452)	72	3.9
3	Kemapoxy 165	80	–

3.3 Specimens' Preparation

All specimens were subjected to room-temperature mixing, casting, and compaction processes. Each specimen was layered thrice, and vibration and compaction were applied using a specialized tool. The top layer was leveled to achieve a smooth surface texture. The specimens were cured in a water tank for 28 days to ensure optimal curing, then transferred to an open-air environment until the scheduled testing date. Fig. 1 illustrates the reinforcement patterns employed in the specimens.

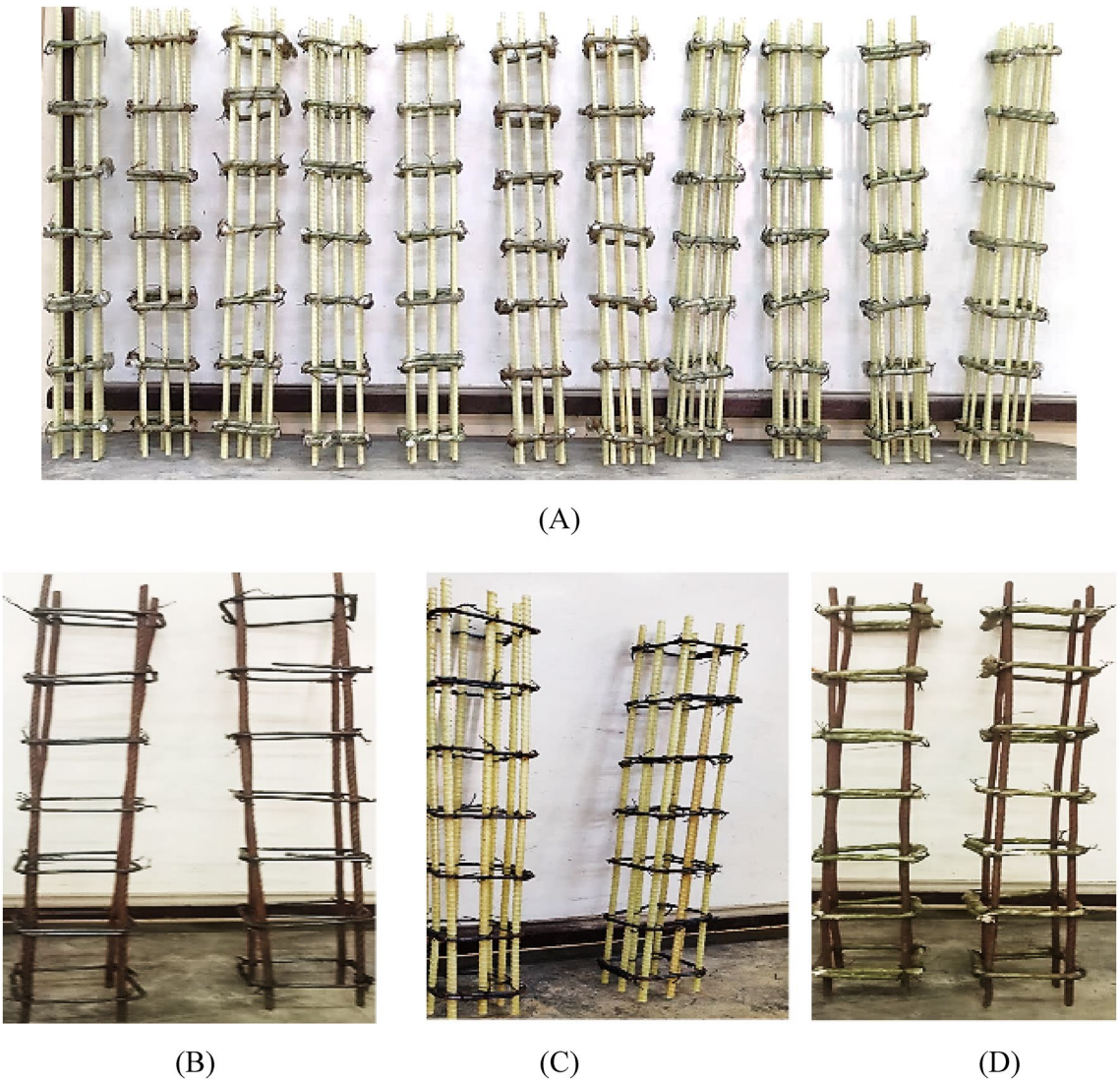

Fig. 1 The reinforcement patterns: **A** full GFRP reinforcement, **B** full steel reinforcement, **C** GFRP longitudinal bars and steel stirrups, and **D** steel longitudinal bars and GFRP stirrups

Twelve columns were reinforced with 8 Φ 10 mm GFRP longitudinal bars and 7 Φ 8 mm stirrups**.** The GFRP stirrups were manually fabricated in the lab and shaped during the casting phase before the resin was fully cured. To ensure equivalent axial stiffness across all tested columns, the steel reinforcement consisted of 4 bars with a diameter of 8 mm, while the GFRP reinforcement comprised 8 bars with a diameter of 10 mm. The remaining six columns were divided into three groups. The first group (two columns) included 4 Φ 8 mm steel bars and 7 Φ 8 mm steel stirrups. The second group (two columns) used 4 Φ 8 mm steel bars and 7 Φ 8 mm GFRP stirrups. The final group (two columns) was reinforced with 8 Φ 10 mm GFRP bars and 7 Φ 8 mm steel stirrups.

Fig. 2 shows the steps for the strengthening of NSM GFRP bars. Firstly, the grooves were meticulously carved into the concrete covers of the tested columns. The slits measure 1.5 times the diameter ("d") of the NSM bars in width and depth, adhering to ACI 440.2R-17 guidelines. Consequently, for GFRP bar diameters expressed as millimeters, a 15-mm slit width was established. After finishing the grooves and cutting them to the required dimensions, epoxy was applied to partially fill them. Subsequently, the rods were carefully positioned, and the outer surface was leveled and polished. Additional adhesive material was applied to saturate the remaining grooves, ensuring optimal adherence. To apply the GFRP layer wrap, begin by using a wire brush to remove loose particles from the surface of the specimen. Next, cut the GFRP woven to the necessary dimensions. Then, mix polyester resin and hardener (peroxide) together for one minute before applying it to the column surface using a paint roller. Afterward, affix the GFRP woven to the column surface, ensuring saturation with polyester. Finally, an overlap in the layers of 15 cm is created, as shown in Fig. 3.

3.4 Test Setup

LVDTs (linear variable differential transducers) with a total measuring range of 50 mm were used to assess the column's vertical and lateral displacements. These LVDTs were securely mounted on the specimen and connected to the loading frame. A hydraulic jack with a capacity of 2000 kN was utilized to apply the loading rate of 30 kN/min. The configurations of the test setup are illustrated in Figs. 4 and 5. As shown in Fig. 4, steel plate caps were used to test the columns illustrated in the figure as column heads. These heads were locally designed to apply axial and eccentric loading to the specimens. In the axial loading case, the plate was centered on the column, while for the eccentric loading, the plates were positioned 30 mm and 60 mm away from the center, respectively. The eccentricity was calculated to ensure the loading path remained within the P–M interaction curve during

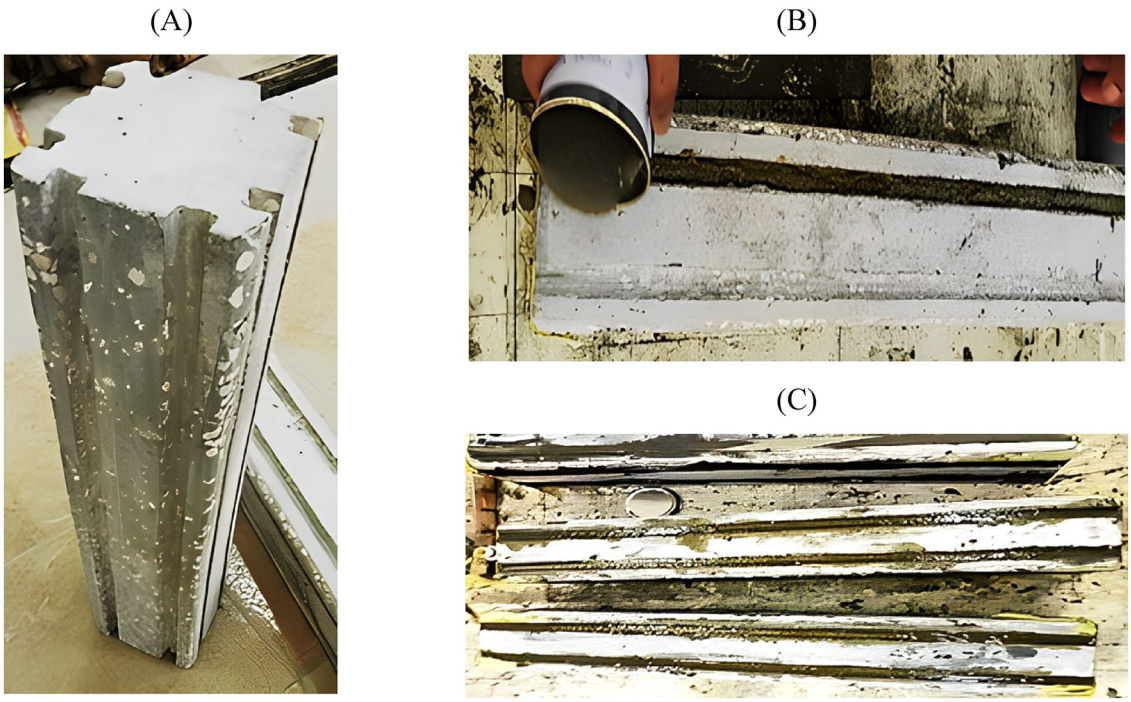

Fig. 2 Strengthening with NSM: **A** the grooves needed to NSM, **B** epoxy is placed in grooves, and **C** putting the NSM strengthening into grooves and leveling the surface

Fig. 3 Strengthening with GFRP wrap

loading and moment application. For all experiments, a Linear Variable Differential Transformer (LVDT) was set up to measure deformations, and an initial load of 10 kN was cautiously applied. This load level was consistently maintained until the column specimen ultimately failed.

4 Results and Discussion

4.1 Control Specimens

The data in Fig. 6a, b show the relationship between axial load, axial displacement, and lateral displacement in the three control specimens, which were reinforced with GFRP as the main reinforcement and stirrups. The results shown in Fig. 5a indicate no significant reduction in the elastic stiffness of specimen Gg-0lay-0-30 compared to Gg-0lay-0-0. However, the maximum load and axial displacement of specimen Gg-0lay-0-30 were approximately 32.5% and 7.3% less than those of specimen Gg-0lay-0-0, respectively. Similarly, the maximum load and axial displacement values of specimen Gg-0lay-0-60 showed a notable reduction of about 71.9% and 35.2%, respectively, compared to specimen Gg-0lay-0-0. The results demonstrate a clear and systematic decrease in the axial bearing capacity of columns as loading eccentricity increases. This reduction in capacity is primarily attributed to the combined effects of the increased bending moment alongside the applied axial load. As the eccentricity grows, the moment arm extends, intensifying the bending stresses within the column. This interaction between bending and axial forces creates significant tensile stresses on the outer fibers of the column section, particularly on the tension side. As the tensile stresses exceed the material's tensile strength, visible cracks form and propagate, compromising the column's integrity. These cracks accelerate the failure process, diminishing the column's ability to carry additional loads and reducing its overall stiffness. Therefore, these tensile cracks initiate a rapid decline in structural capacity, often leading to brittle failure modes under high-eccentricity loads. These findings align closely with the conclusions of other studies in the field, which have reported similar reductions in load-bearing capacity and observed rapid failure patterns in columns under eccentric loading conditions due to the compounding effects of axial and bending forces. This correlation strengthens the validity of our results and highlights the importance of considering loading eccentricity in the design and reinforcement of short (Aslam et al., 2021; Elchalakani & Ma, 2017; Elchalakani et al., 2017; Gao et al., 2021; Wang et al., 2024).

As seen in Fig. 6b, the various lateral displacements found in the widths of the three samples show the effect of increased eccentricity, particularly in specimens Gg-0lay-0-60, which failed under the loading head. The increase in loading eccentricity prevents the column cross-section from lateral deformation. Fig. 7a–c shows the failure modes observed in the control specimens. Specimen Gg-0lay-0-0 suffered complete failure upon hearing reinforcing bars cracking, followed by the failure of concrete covers. In contrast, specimen Gg-0lay-0-30 exhibited transverse cracks on the tension side and longitudinal cracks on the compression side, with no concrete detachment, even when the load decreased to less than 80%. The specimen Gg-0lay-0-60, loaded near the edge of

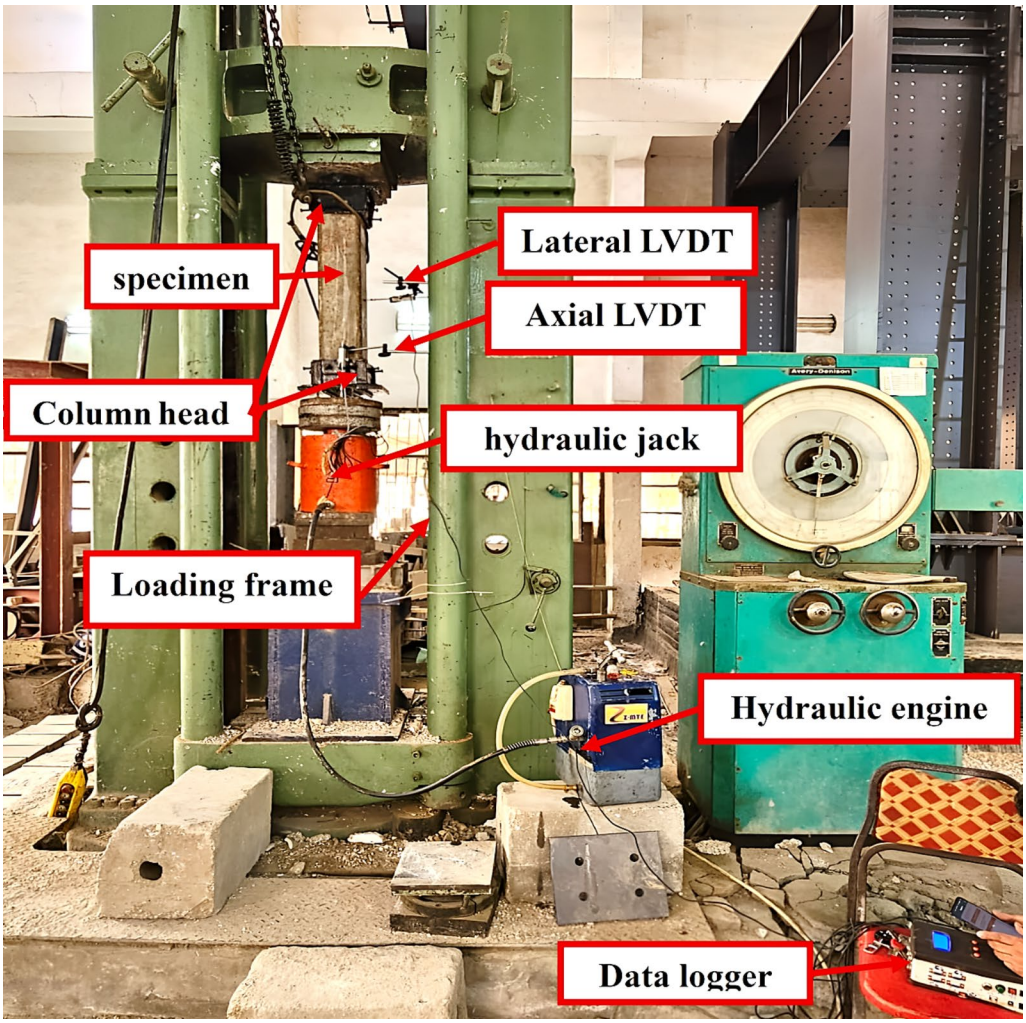

Fig. 4 The test setup and instruments

the column and subjected to an eccentricity of 60, failed in a manner resembling fragmentation below the loading head. It failed under the load without a notable decrease in load after reaching its maximum capacity.

4.2 Effect of Different Types of Reinforcement

Three sets of specimens were prepared to assess the performance of GFRP reinforcement compared to steel: Ss-0lay-0-0 and Ss-0lay-0-30, reinforced with steel longitudinal bars and stirrups; Gs-0lay-0-0 and Gs-0lay-0-30: reinforced with GFRP longitudinal bars and steel stirrups; Sg-0lay-0-0 and Sg-0lay-0-30: reinforced with steel longitudinal bars and GFRP stirrups. Fig. 8 presents the relationship between axial load, axial displacement, and lateral displacement for these four specimen types. Fig. 8a and b shows that the elastic stiffness of the Sg-0lay-0-0 and Gs-0lay-0-0 specimens is comparable to that of the Gg-0lay-0-0 specimens. However, the Ss-0lay-0-0 specimen exhibits higher elastic stiffness than the Gg-0lay-0-0 specimen. Furthermore, the Ss-0lay-0-0 specimen exhibited a slight reduction in maximum load by 6% and axial displacement by 7% compared to the Gg-0lay-0-0 specimen but an 8% increase in lateral displacement. These results proved that the performance of columns reinforced with GFRP is comparable to those reinforced with steel, especially considering that the GFRP-reinforced columns used only one-third of the steel reinforcement.

GFRP has a low modulus of elasticity compared to steel reinforcement, which limits its ability to deform adequately when subjected to load. Therefore, before using GFRP, the element must be properly designed. It must not just be substituted for steel with the same quantity; the displacement for both materials should be equal. The Gs-0lay-0-0 specimen exhibited a 16% decrease in maximum load and a 22% decrease in

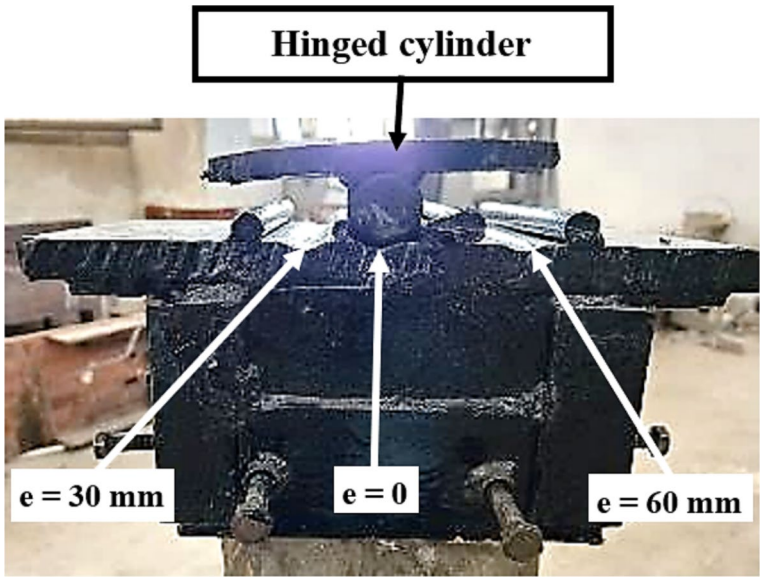

Fig. 5 Configurations of the steelhead loading plate

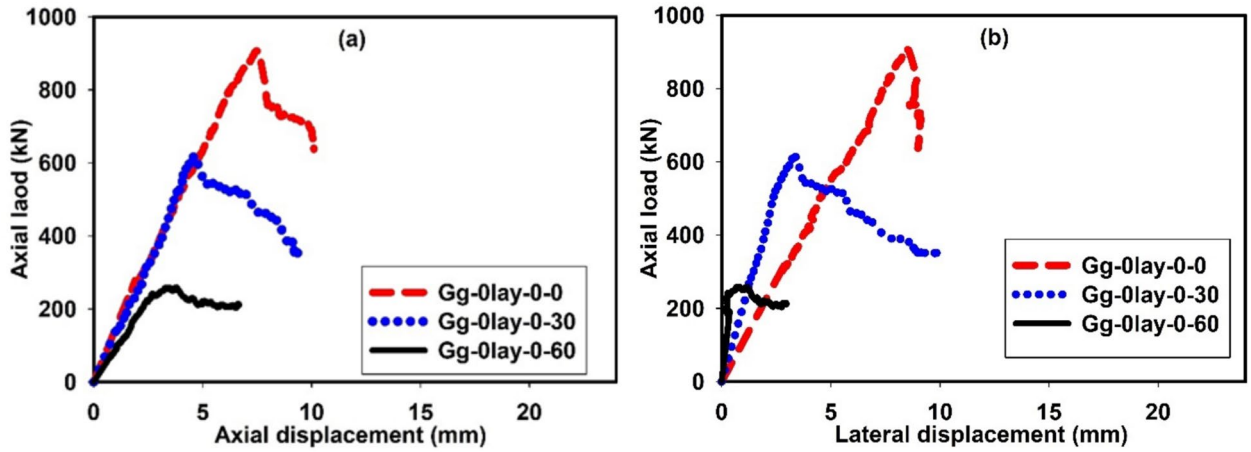

Fig. 6 Results of control columns: **a** axial load–axial displacement, **b** axial load–lateral displacement

maximum axial displacement compared to the Gg-0lay-0-0 specimen. However, it displayed a significant 129% increase in lateral displacement. This behavior can be attributed to the greater elongation of steel than GFRP, leading to insufficient confinement of the longitudinal GFRP reinforcement. This lack of confinement resulted in longitudinal cracking and reduced axial load capacity. In contrast, the Sg-0lay-0-0 specimen showed only a slight decrease in maximum load (8%) and axial displacement (10%) compared to the Gg-0lay-0-0 specimen, with no significant increase in lateral displacement. This difference can be attributed to the combined effect of the steel stirrups, longitudinal steel reinforcement, and the restraining influence of the GFRP stirrups on the longitudinal steel rebar.

Under an eccentric load of 30 mm, as shown in Fig. 8c and d, the behavior of the specimens changed. The Ss-0lay-0-30 specimen exhibited a 10% increase in peak load, a 150% increase in axial displacement, and a 25% increase in lateral displacement compared to the steel-reinforced specimen. Similarly, the Sg-0lay-0-30 specimen showed a 5% increase in peak load, a 150% increase in axial displacement, and a 50% increase in lateral displacement compared to the Gg-0lay-0-30 specimen.

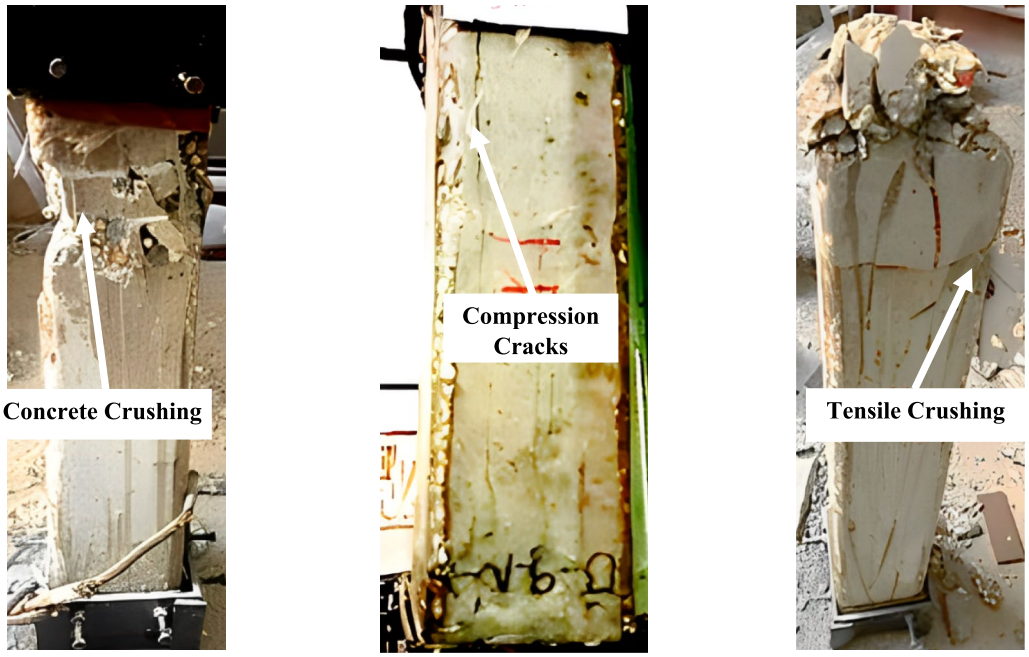

Fig. 7 Mode of failure for control columns: **a** specimen Gg-0lay-0-0, **b** specimen Gg-0lay-0-30, **c** specimen Gg-0lay-0-60

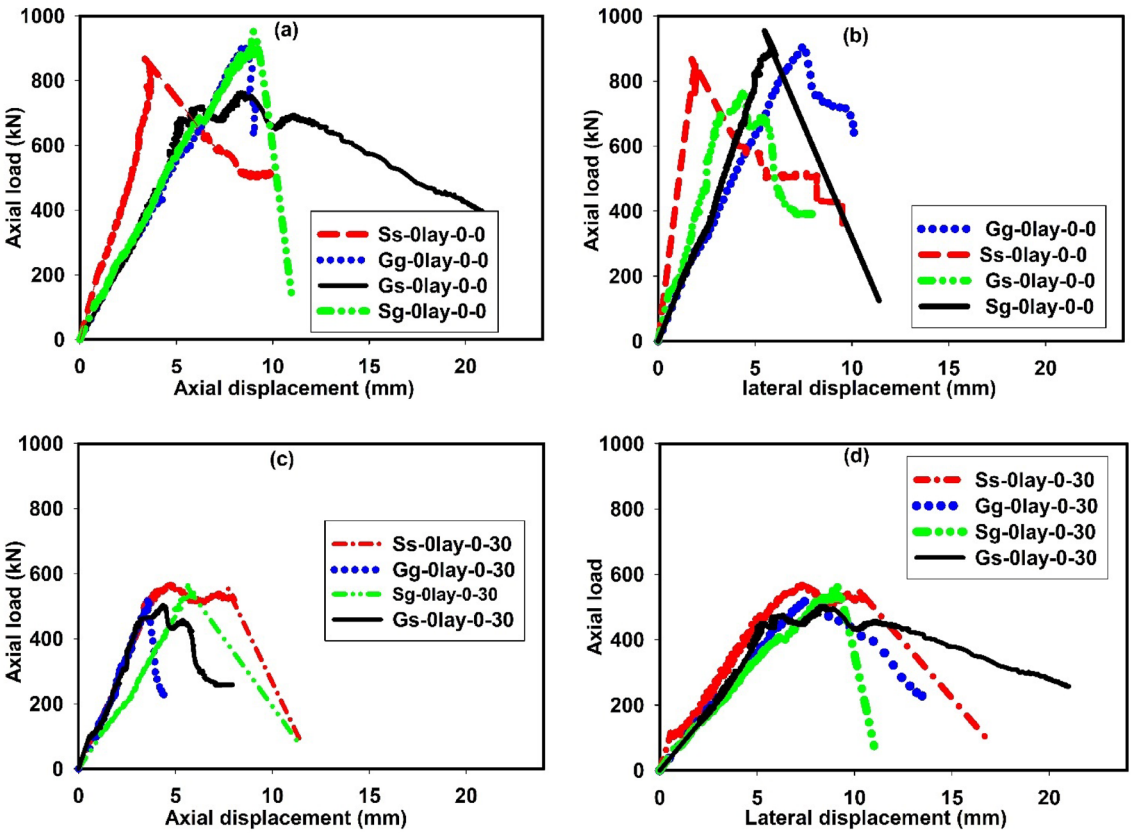

Fig. 8 Results for the effect of reinforcing type: **a** axial load–axial displacement; **b** axial load–lateral displacement at $e = 0$; **c** axial load–axial displacement; **d** axial load–lateral displacement at $e = 30$ mm

These enhancements can be attributed to steel's higher modulus of elasticity than GFRP, enabling the specimens to sustain greater loads and exhibit more elastic behavior. Fig. 9 illustrates various failure modes. The Ss-0lay-0-0 specimen, Fig. 9a, failed due to compressive zone collapse and lateral cracking. The Sg-0lay-0-0 specimen, Fig. 9b, exhibited a similar failure mode. However, the Gs-0lay-0-0 specimen, Fig. 8c, failed due to longitudinal cracking, exacerbated by the lack of support from the longitudinal GFRP rebar. Finally, Fig. 9d–f shows a combined failure mode involving compressive zone collapse, lateral cracking, and local buckling.

4.3 Effect of Strengthening by One Layer of GFRP Wrap

Fig. 10 illustrates the impact of eccentricity on the performance of GFRP-strengthened columns with a single layer. Fig. 10a shows the relationship between axial load and axial displacement, while Fig. 10b depicts the relationship between axial and lateral displacement. Specimen Gg-1lay-0-0 was centrally loaded, Gg-1lay-0-30 had an eccentricity of 30 mm, and Gg-1lay-0-60 had an eccentricity of 60 mm. While the elastic stiffness of Gg-1lay-0-30 remained comparable to Gg-1lay-0-0, it exhibited significant reductions in maximum load, axial displacement, and lateral displacement by approximately 36%, 28%, and 17%, respectively. For Gg-1lay-0-60, the impact of eccentricity was even more pronounced, with reductions of 2%, 59%, 55%, and 40% in elastic stiffness, maximum load, axial displacement, and lateral displacement, respectively. These findings highlight the detrimental effect of eccentricity on the axial load-carrying capacity of strengthened columns. The combined action of axial load and bending moment induced by eccentricity leads to tensile stresses, resulting in crack formation and premature failure. This observation aligns with previous research (Abd el-Hafez et al., 2023; Benzaid et al., 2008; Patel et al., 2022; Sai Madupu & Sai Ram, 2021; Samy et al., 2022). The slight increase in lateral displacement with increasing eccentricity is attributed to the induced bending moment.

Fig. 11a–c shows the failure modes of the tested specimens. Specimens Gg-1lay-0-0 and Gg-1lay-0-30 failed at the edge due to cutting in the GFRP wrap without affecting the entire cross-section. This failure mode can be attributed to the higher values of lateral displacement observed in these specimens. In contrast, Gg-1lay-0-60 failed due to a cut in the wrap at the upper end, leading to a concrete collapse in that region.

4.4 Effect of Strengthening by Three Layers of GFRP Wrap

The data presented in Fig. 12a and b illustrate the relationship between axial load, axial displacement, and lateral displacement for three GFRP-wrap specimens subjected to varying eccentricities. Specimen Gg-3lay-0-0 was centrally loaded, Gg-3lay-0-30 had an eccentricity of 30 mm, and Gg-3lay-0-60 had an eccentricity of 60 mm. A notable observation is the absence of a reduction in elastic stiffness for specimens Gg-3lay-0-30 and Gg-3lay-0-60 compared to Gg-3lay-0-0. However, increasing eccentricity led to significant decreases in maximum load and axial displacement. Specifically, Gg-3lay-0-30 exhibited a 34% and 20% reduction, respectively, while Gg-3lay-0-60 showed a more substantial reduction of 55% and 4%. Conversely, lateral displacement increased by 53% and 15%, respectively. These results highlight the detrimental impact of eccentricity on the axial capacity of columns. The combined axial load and bending moment induced by eccentricity results in tensile stresses, leading to crack formation and premature failure. This finding corroborates previous research (Kumutha et al., 2007; Raval & Dave, 2013), where increased eccentricity was linked to amplified lateral displacement and reduced load-carrying capacity.

The failure modes observed in Fig. 13a–c further elucidate the effect of eccentricity. For Gg-3lay-0-0, failure was dominated by wrap resistance, resulting in concrete fragmentation at the wrap cut. In Gg-3lay-0-30, a longitudinal crack developed in the compression wrap zone, ultimately leading to failure. Conversely, Gg-3lay-0-60 experienced minimal damage, with failure occurring below the column due to a combination of wrap and concrete crushing. This failure mode is consistent with previous studies (Abd el-Hafez et al., 2023; Hussain et al., 2024; Kumutha et al., 2007; Patel et al., 2022; Raval & Dave, 2013; Samy et al., 2022).

4.5 Effect of Strengthening with Three Layers of GFRP Wrap and NSM Bars

Fig. 14 illustrates the impact of strengthening columns with three layers of GFRP wrap and NSM GFRP bars. Fig. 14a shows the relationship between axial load and axial displacement, while Fig. 14b presents the relationship between axial load and lateral displacement for three specimens tested under varying eccentricities. The first specimen was centrally loaded, the second had an eccentricity of 30 mm, and the third had an eccentricity of 60 mm. The elastic stiffness of the Gg-3lay-N-30 specimen was comparable to that of the Gg-3lay-N-0 specimen. However, the maximum load, axial displacement, and maximum lateral displacement of the Gg-3lay-N-30 specimen were reduced by 19%, 23%, and 11%, respectively, compared to the Gg-3lay-N-0 specimen. Similarly, the Gg-3lay-N-60 specimen exhibited no reduction in elastic stiffness compared to the Gg-3lay-N-0 specimen. However, it showed significant reductions in maximum load, axial displacement,

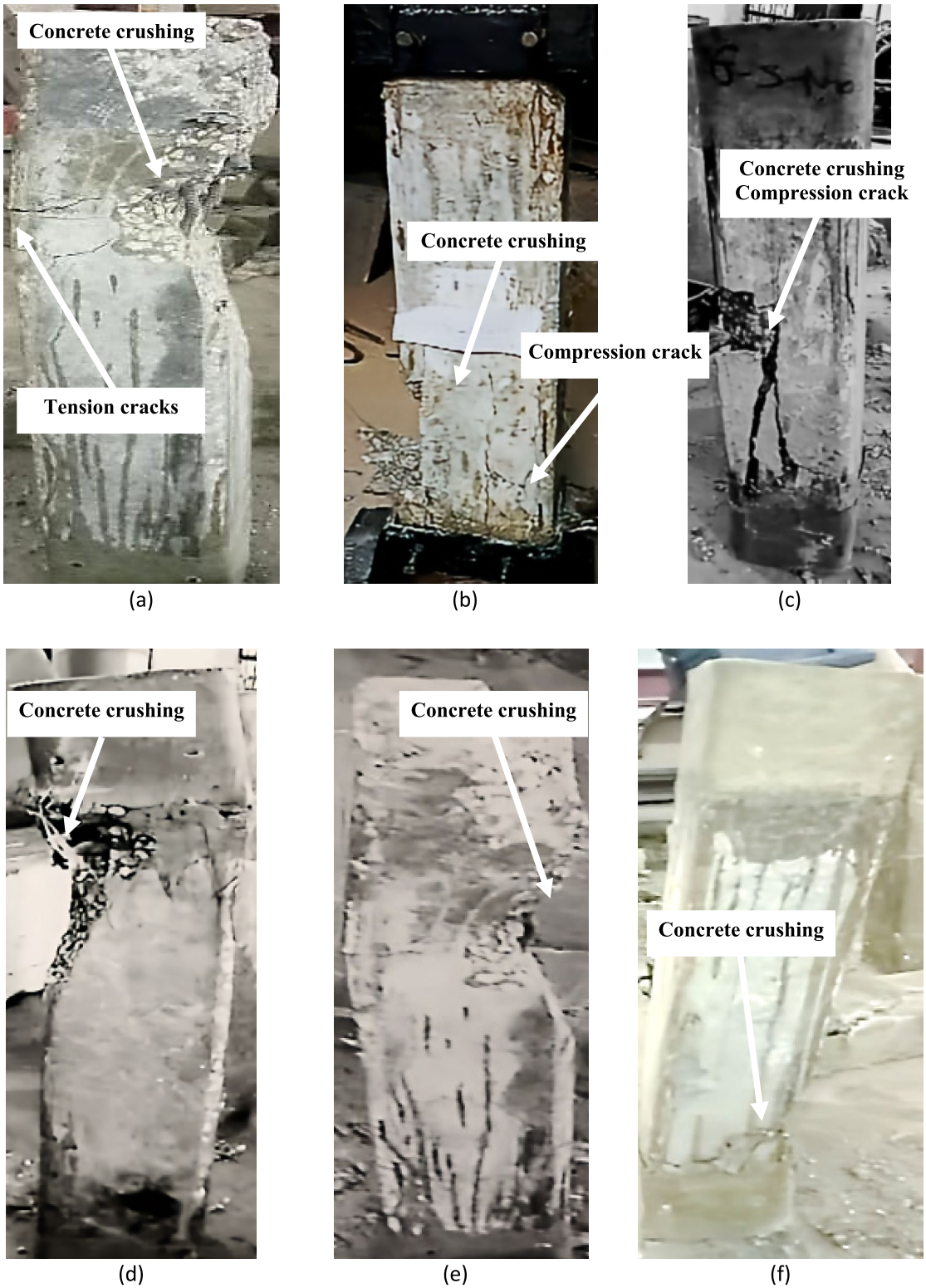

Fig. 9 Mode of failure: **a** specimen Ss-0lay-0-0, **b** specimen Sg-0lay-0-0, **c** specimen Gs-0lay-0-0, **d** specimen Ss-0lay-0-30, **e** specimen Sg-0lay-0-30, **f** specimen Gs-0lay-0-30

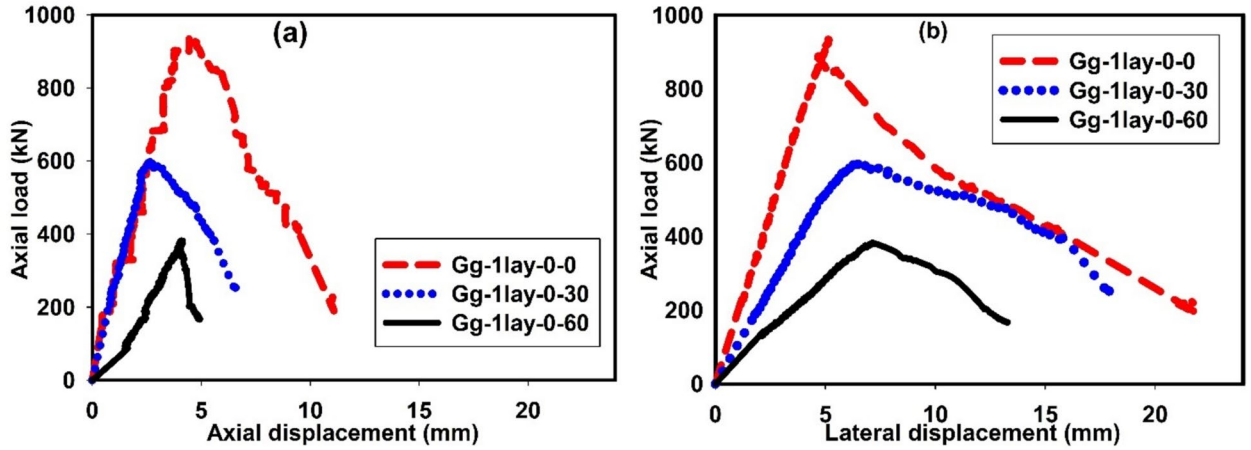

Fig. 10 Results for the effect of one-layer wrap: **a** axial load–axial displacement, **b** axial load–lateral displacement

Fig. 11 Mode of failure: **a** for the specimen G-g-1 lay-0, **b** for the specimen G-g-1 lay-30, **c** for the specimen G-g-1 lay-60

and lateral displacement of 50%, 87%, and 39%, respectively, compared to the (Gg-1lay-0-0) specimen. These findings indicate that increasing the loading eccentricity reduces the axial load-carrying capacity of the columns due to the combined effects of bending moment and axial load, leading to tensile cracking. This observation aligns with previous research (Chellapandian et al., 2017, 2019; Eshaghi-Milasi et al., 2002; Moshiri et al., 2015).

Fig. 15 shows the failure mode in specimens strengthened by NSM and three layers of GFRP wraps. Fig. 15a shows that the failure mode in the specimen Gg-3lay-N-0 occurred due to increased compression in the NSM bar, leading to buckling inside the bars. Consequently, desponding in the bar and cuts in both the bars

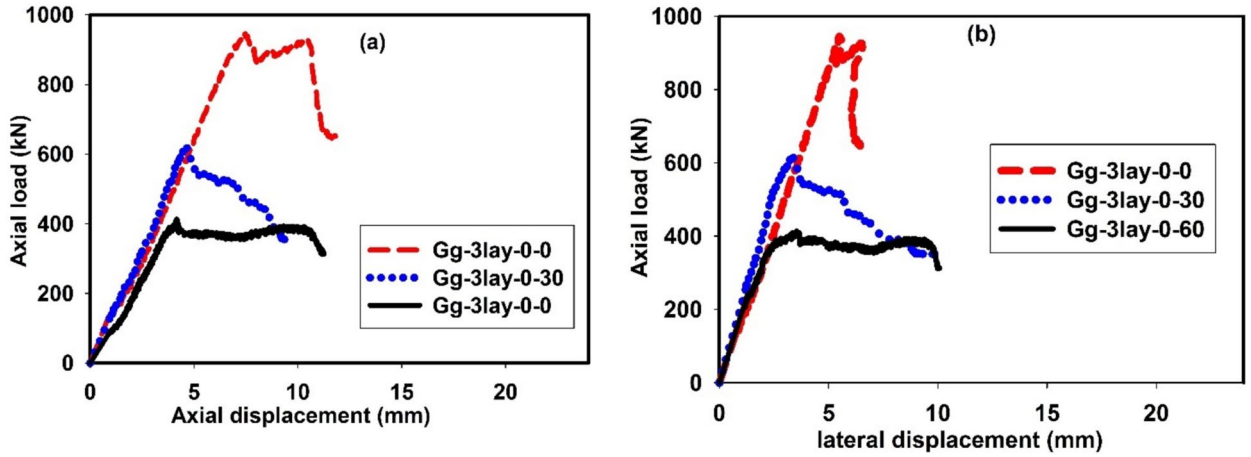

Fig. 12 Results for the effect of three layers wrap: **a** axial load–axial displacement, **b** axial load–lateral displacement

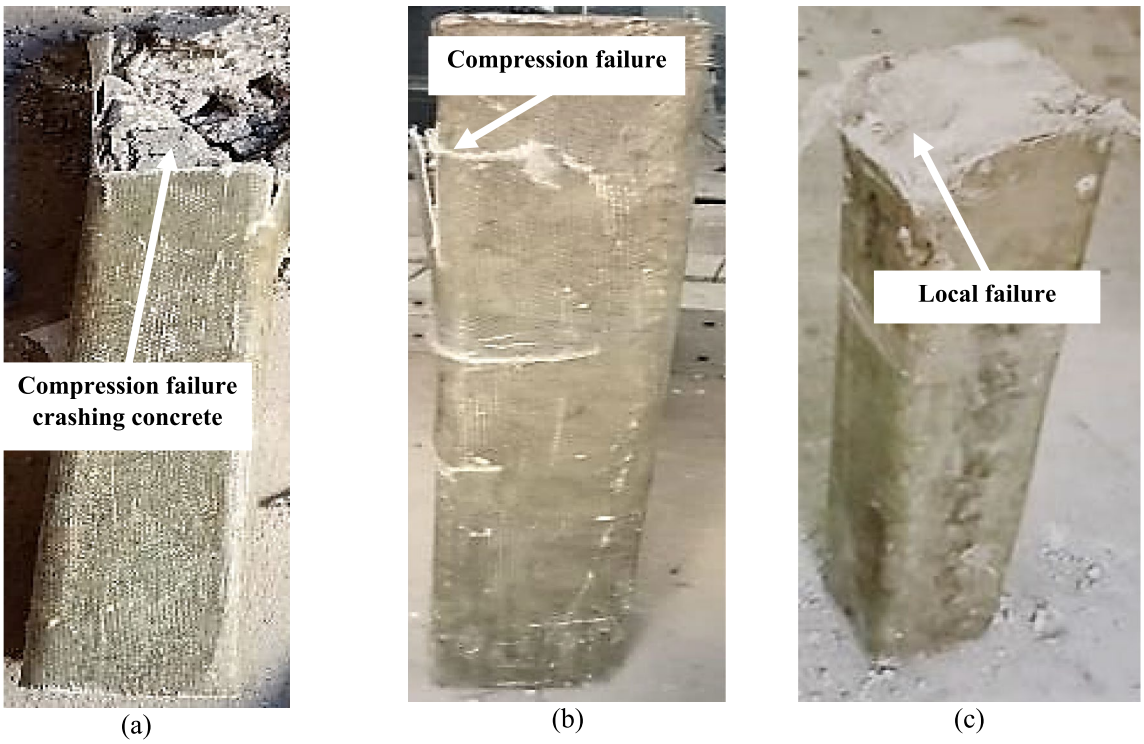

Fig. 13 Mode of failure: **a** for the specimen Gg-3lay-0-0, **b** for the specimen Gg-3lay-0-30, **c** for the specimen Gg-3lay-0-60

and GFRP layers were observed. In Fig. 15b, for specimen Gg-3lay-N-30, failure occurred with cuts specifically in the GFRP layers within the compression zone of the longitudinal cut. Notably, this failure did not involve any defects in the NSM. Finally, Fig. 15c shows the failure mode for the specimen Gg-3lay-N-60, in which failure occurred in the compression zone at the load head. It is important to note that there was no damage to the overall specimen, consistent with the failure mode observed in previous studies (Chellapandian et al., 2017, 2019).

4.6 *Comparison Between the Strengthening Techniques Used at e = 0*

This section will compare and analyze the performance differences between the control specimens and those reinforced with GFRP under concentric loading conditions $e=0$. All specimens were strengthened with GFRP.

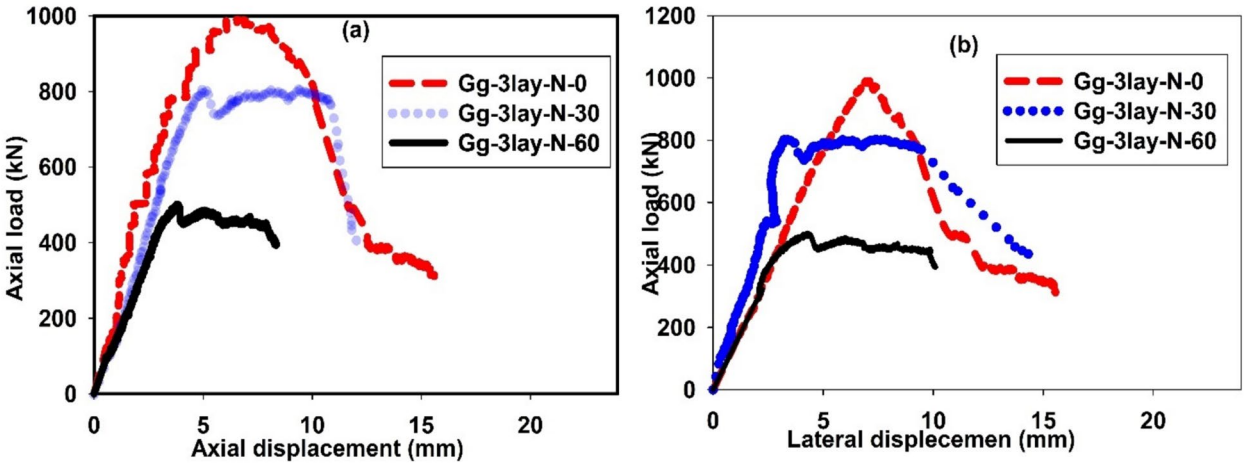

Fig. 14 Results for the effect of three layers wrap and NSM bars: **a** axial load–axial displacement, **b** axial load–lateral displacement

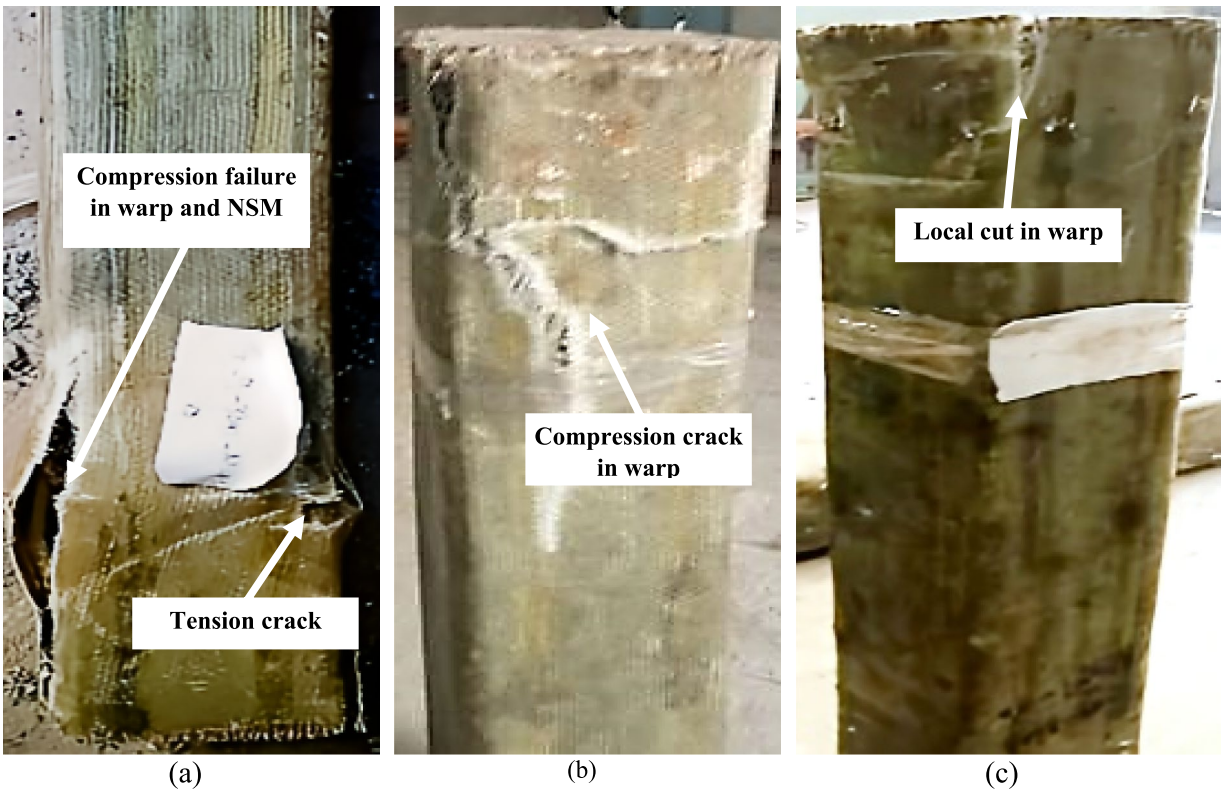

Fig. 15 Mode of failure: **a** for the specimen Gg-3lay-N-0, **b** for the specimen Gg-3lay-N-30, **c** for the specimen Gg-3lay-N-60

Fig. 16a and b illustrates the relationship between the applied load and resulting axial and lateral displacements. The Gg-1lay-0-0 specimen exhibited a 3% increase in compressive load capacity and a 10% increase in axial displacement compared to the control Gg-0lay-0-0 specimen. Notably, the (Gg-1lay-0-0) specimen demonstrated improved failure behavior, avoiding concrete cover debonding observed in the control specimen, Fig. 16a.

The Gg-3lay-0-0 specimen showed a more significant 4% increase in compressive load and an 11% increase in axial displacement. However, its failure mode was characterized by wrap failure, leading to concrete damage and collapse, a behavior not observed in the control

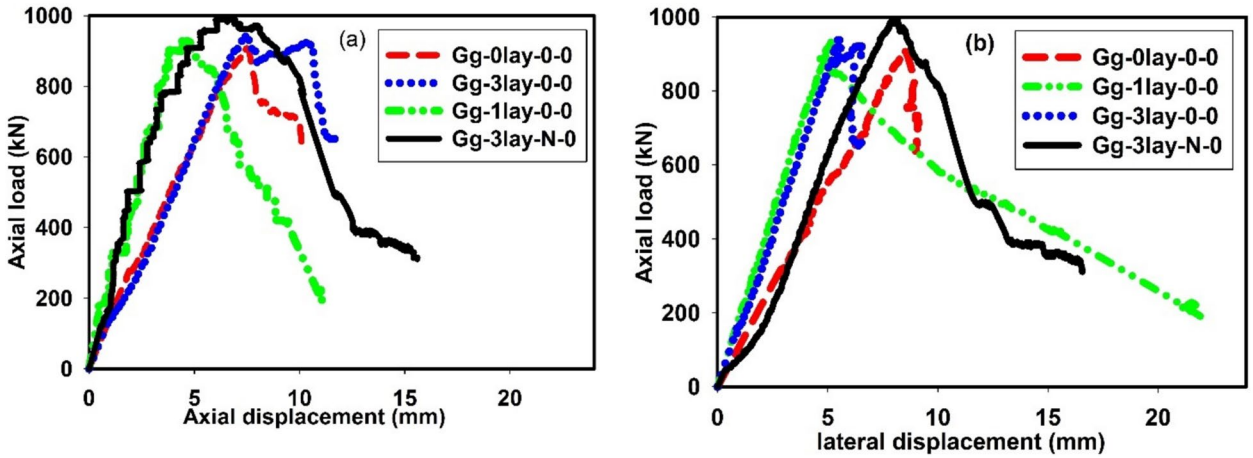

Fig. 16 Comparison of strengthening techniques at $e = 0$: **a** axial displacement and **b** lateral displacement

specimen. The Gg-3lay-N-0 specimen exhibited the most substantial improvement, with a 10% increase in loading capacity and a 49% increase in axial displacement compared to the control. This enhanced performance can be attributed to the hybrid system combining NSM bars with three layers of GFRP wrapping. This system effectively increased the load-bearing capacity and prevented the lateral displacement of the NSM bars and the concrete. In some cases, the lack of a significant increase in ultimate load capacity is primarily due to the limitations imposed by the concrete's capacity to carry axial load. As the load approaches its maximum capacity, the longitudinal fibers limit lateral displacement and induce significant tensile stresses. The presence of NSM bars allows a substantial portion of the load to be transferred to the steel reinforcement, enabling the column to undergo greater deformation and accommodate larger displacements, ultimately leading to a notable increase in load-carrying capacity.

4.7 *Comparison Between the Strengthening Techniques Used at e = 30 and 60*

A comparison of the strengthening techniques employed at eccentricities of 30 mm and 60 mm is presented in Fig. 17. Fig. 17a and b illustrates the relationship between axial load and axial and lateral displacements at an eccentricity of 30 mm. The data compare three strengthening techniques with control specimens. The Gg-1lay-0-30 specimen exhibited a 16% increase in peak load and a 48% increase in total axial displacement compared to the control specimen. The Gg-3lay-0-30 specimen demonstrated a 20% improvement in maximum load and a 100% increase in total axial displacement. The Gg-3lay-0-30 specimen showed the most significant improvement, with a 56% enhancement in ultimate load and a 170% increase in total axial displacement.

Fig. 17c and d depicts the relationship between axial load and axial and lateral displacements at an eccentricity of 60 mm. The Gg-1lay-0-60 specimen showed a 47% improvement in peak load, while the Gg-3lay-0-60 specimen exhibited a 60% improvement. The Gg-3lay-N-60 specimen demonstrated the most significant improvement, with a 93% increase in peak load. Under eccentric loading, the column's cross-section is divided into compression and tension zones. The GFRP wrap reinforcement effectively strengthens the column in both directions, preventing lateral deformation in the compression zone and controlling crack initiation and propagation in the tension zone. Increasing the number of wrap layers enhances these beneficial effects. Moreover, increasing the eccentricity distance amplifies the impact of the wrap reinforcement due to the reduced compression zone area. In a hybrid strengthening system, the NSM bars provide additional reinforcement in both tension and compression zones, while the GFRP wrap confines these bars, further enhancing the column's capacity to resist cracking and deformation.

4.8 Performance of GFRP-Strengthened Columns Under Concentric and Eccentric Loading

This study investigates the effectiveness of various GFRP strengthening techniques on the behavior of reinforced concrete columns under concentric and eccentric loading conditions. The performance of columns reinforced with a single layer of GFRP, three layers of GFRP, and a combination of three layers of GFRP and NSM GFRP bars was evaluated. Table 4 shows the load and ductility percentage improvement performance for each strengthening

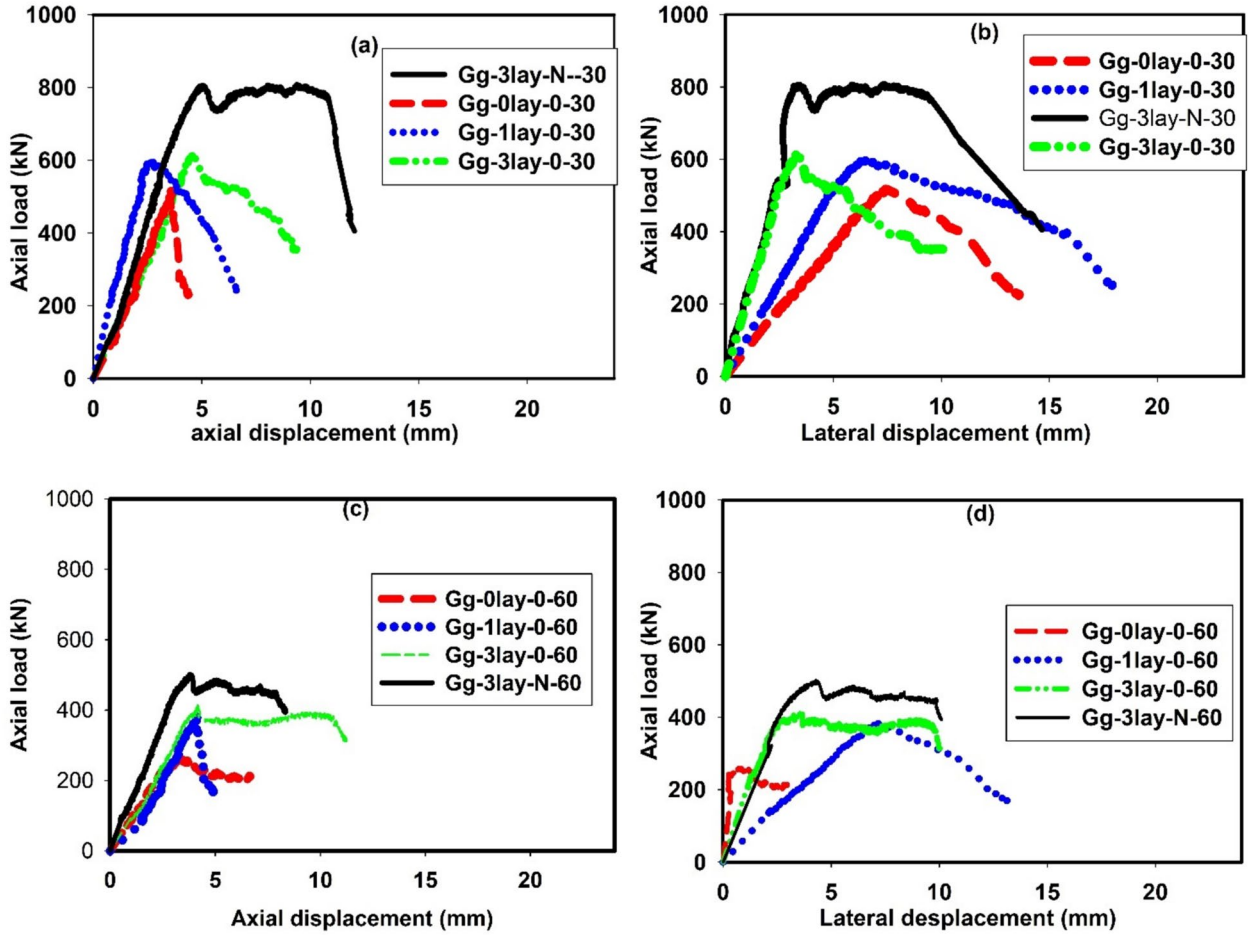

Fig. 17 Comparison between the strengthening techniques used: **a** and **b** for $e = 30$ mm and **c** and **d** for $e = 60$ mm

Table 4 The load and ductility percentage improvement performance for each strengthening technique

Eccentricity	Specimens' property	Percent of improvement		
		One layer (%)	Three layers (%)	Three-layers + 8-bar NSM (%)
$e = 0$	Load capacity	2.9	4	10
	Failure axial displacement	9.1	17	55
	Failure lateral displacement	130	− 28.32	80.39
$e = 30$	Load capacity	16	20	56
	Failure axial displacement	47.75	111	170
	Failure lateral displacement	32	− 24.7	7.3
$e = 60$	Load capacity	48	60	93
	Failure axial displacement	− 26	68.6	25
	Failure lateral displacement	350	240	240

technique. This percentage is calculated by comparing it to the control specimen.

Columns reinforced with a single layer of GFRP showed limited load-carrying capacity and stiffness improvements compared to control specimens. The axial load

increased by 2.9% at $e=0$, 16% at $e=30$, and 48% at $e=60$. Moreover, a significant increase in lateral displacement was observed, raising concerns about structural stability. The effectiveness of single-layer GFRP reinforcement was further diminished under increasing eccentric loading conditions; the lateral displacement increased by 130% at $e=0$, 32% at $e=30$, and 350% at $e=60$. Three-layer GFRP reinforcement significantly improved the load-carrying capacity and stiffness of the columns while mitigating the increase in lateral displacement. This technique proved particularly effective in resisting eccentric loading. The increased confinement provided by multiple layers of GFRP reduced lateral deformation and enhanced overall performance; the axial load increased by 4% at $e=0$, 20% at $e=30$, and 60% at $e=60$ compared to the control specimen.

Combining three layers of GFRP with NSM bars, the hybrid strengthening technique provided the most significant enhancement in load-carrying capacity and stiffness; the axial load is increased by 10% at $e=0$, by 56% at $e=30$, and by 93% at $e=60$ compared to the control specimens. The NSM bars contributed to increased load-carrying capacity by providing additional reinforcement in tension, while the GFRP wrap restrained concrete and prevented excessive cracking. This hybrid approach proved particularly effective for eccentrically loaded columns, offering enhanced resistance to bending moments and axial loads and substantially increasing load-carrying capacity and stiffness. While the three-layer GFRP reinforcement improved the performance of the columns, the hybrid strengthening technique with NSM bars provided superior results, particularly under eccentric loading conditions. Combining the two techniques offers a robust solution for strengthening reinforced concrete columns and can be considered for practical applications (Chellapandian et al., 2017; Imjai et al., 2022; Sai Madupu & Sai Ram, 2021; Sun et al., 2017). In paper 11, peak load performance improved by 32% with one layer, 47.7% with two layers, and 46.85% with three layers under concentric loading compared to control. In paper 14, peak load increased by 15% with one layer and 31.35% with two layers under concentric loading compared to control. Paper 35 utilized a hybrid system with 8 NSM CFRP laminate strips and two layers of CFRP fabric, achieving a peak load increase of 25.5% and a failure displacement increase of 163% under concentric loading. Paper 38 demonstrated that the NSM strengthening solution enhanced the ultimate load-carrying capacities of strengthened beams by up to 64%.

4.9 Axial Load–Bending Moment Interaction Curve

The test specimens in this study were categorized into four groups based on their reinforcement configurations. The first category, Gg-0lay-0, was the control specimen with no additional strengthening. The second category, Gg-1lay-0, consisted of specimens strengthened with a single wrap layer. The third category, Gg-3lay-0, included specimens reinforced with three wrap layers. Lastly, the Gg-3lay-N specimens were strengthened with three wrap layers and further reinforced with eight near surface-mounted (NSM) rebars.

Each category consists of three specimens, differentiated by varying load eccentricities of 0 mm, 30 mm, and 60 mm. In Fig. 18, the effectiveness of strengthening

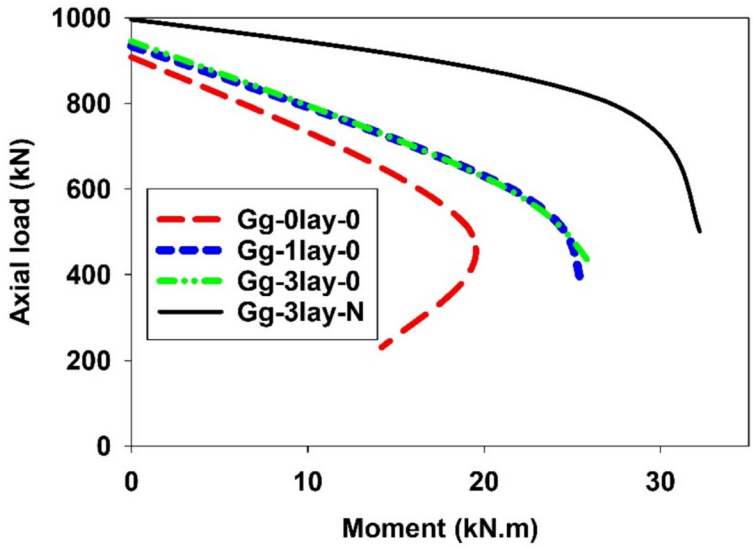

Fig. 18 Comparison of the P–M interaction curves of the control and strengthen specimens

improves as the load eccentricity increases, up to the point where the load is balanced in the P–M curves. This is shown by comparing the strengthened and control specimens. The improvement in strengthening under eccentric load occurs by increasing the specimen's resistance to the loaded moment and keeping the specimen in compression. In the hybrid system, the improvement is increased because the reinforcement specimen is subject to tension and compression, which prevents the NSM from breaking. The insights gained from this study have significant practical implications. During the design phase, understanding the effects of load eccentricity can be incorporated into the axial load effect, providing a better understanding of the soil–structure system and leading to improvements in both structural efficiency and safety. Load eccentricity is particularly important for tall buildings, where lateral loads are particularly influential, generating significant bending moments in the columns. It also plays a crucial role in the design of tall bridges.

5 Conclusions

The experimental results presented in this work reveal the following conclusions:

1- As the loading eccentricity increases, the axial capacity of a column diminishes considerably. For instance, an $e=30$ eccentricity reduces the maximum load by approximately 43%, and an $e=60$ eccentricity leads to a significant 71% reduction on the sum specimen type.
2- Our results show that columns fully reinforced with GFRP exhibit comparable performance to those reinforced fully with steel or a hybrid combination. However, using GFRP for longitudinal reinforcement and steel for stirrups resulted in a 16% reduction in axial load, a 22% reduction in axial displacement, and a 129% increase in lateral displacement compared to fully GFRP-reinforced columns.
3- Adding a GFRP wrap to a reinforced specimen significantly improves its mechanical properties, particularly at increased eccentricity. Specifically, compared to the control specimen, the axial load increased by 2.9% at $e=0$, 16% at $e=30$, and 48% at $e=60$.
4- The application of three layers of GFRP wrap significantly improves the mechanical properties of a specimen, particularly at increased eccentricity. Specifically, the axial load increased by 4% at $e=0$, 20% at $e=30$, and 60% at $e=60$ compared to the control specimen.
5- Combining NSM GFRP rebars and GFRP wrap can significantly increase the loading capacity and improve displacement ductility. The obtained results show that these specimens outperform others. For example, the axial load is increased by 10% at $e=0$, by 56% at $e=30$, and by 93% at $e=60$ compared to the control specimens.
6- Strengthening is more effective as the load eccentricity increases up to the point where the load is balanced in the P–M curves. This is demonstrated by comparing the enhanced and control specimens. Strengthening under eccentric load is improved by enhancing the specimen's resistance to the loaded moment and maintaining compression.

Acknowledgements
This work represents the second author's experimental portion of the M.Sc. thesis.

Author contributions
A A: writing original draft, validation, supervision. H E: visualization, supervision, investigation, conceptualization. M Y: writing original draft, methodology, investigation, formal analysis, data curation. M Z: methodology, data curation. S A: validation, supervision, methodology, conceptual.

Funding
Open access funding provided by The Science, Technology & Innovation Funding Authority (STDF) in cooperation with The Egyptian Knowledge Bank (EKB).

Availability of data and materials
All the data required are reported in this manuscript.

Declarations

Ethics approval and consent to participate
Informed consent was obtained from all individual participants included in this study.

Consent for publication
All the authors agree that the article will be published after acceptance.

Competing interests
The authors declare that they have no competing interests.

Author details
[1]Engineering Materials Department, Zagazig University, Zagazig 44519, Egypt. [2]Structural Engineering Department, Faculty of Engineering, Zagazig University, Zagazig 44519, Egypt. [3]Civil and Environmental Engineering, University of Missouri, Columbia, MO 65211, USA.

Received: 12 July 2024 Accepted: 3 February 2025
Published online: 29 April 2025

References

Abd El-Hafez, L. M., Mahmoud, F. R., Fahmy, N. G., & Tawfic, Y. R. (2023). Behavior of large-scale columns strengthened with basalt fiber-reinforced polymers sheets or bars and hybrid FRPs. *Case Studies in Construction Materials, 19*, e02125. https://doi.org/10.1016/j.cscm.2023.e02125

Abdelazim, W., Mohamed, H. M., & Benmokrane, B. (2020). Inelastic second-order analysis for slender GFRP-reinforced concrete columns: Experimental investigations and theoretical study. *Journal of Composites for Construction*. https://doi.org/10.1061/(asce)cc.1943-5614.0001019

Afifi, M. Z., Mohamed, H. M., & Benmokrane, B. (2014). Axial capacity of circular concrete columns reinforced with GFRP bars and spirals. *Journal of Composites for Construction, 18*(1), 04013017. https://doi.org/10.1061/(ASCE)CC.1943-5614.0000438

AlAjarmeh, O. S., Manalo, A. C., Benmokrane, B., Karunasena, W., & Mendis, P. (2019). Axial performance of hollow concrete columns reinforced with GFRP composite bars with different reinforcement ratios. *Composite Structures, 213*, 153–164. https://doi.org/10.1016/j.compstruct.2019.01.096

AlAjarmeh, O. S., Manalo, A. C., Benmokrane, B., Karunasena, W., & Mendis, P. (2020). Effect of spiral spacing and concrete strength on behavior of GFRP-reinforced hollow concrete columns. *Journal of Composites for Construction*. https://doi.org/10.1061/(asce)cc.1943-5614.0000987

Aslam, H. M. U., Khan, Q., Sami, A., & Raza, A. (2021). Axial compressive behavior of damaged steel and GFRP bars reinforced concrete columns retrofitted with CFRP laminates. *Composite Structures, 258*, 113206. https://doi.org/10.1016/j.compstruct.2020.113206

Benzaid, R., Chikh, N.-E., & Mesbah, H. (2008). Behaviour of square concrete column confined with GFRP composite warp/Kompozitiniais stiklo pluoštu armuoto polimero lakštais sustiprintų kvadratinių betoninių kolonų elgsena. *Journal of Civil Engineering and Management, 14*(2), 115–120. https://doi.org/10.3846/1392-3730.2008.14.6

Chellapandian, M., Prakash, S. S., & Sharma, A. (2019). Experimental investigations on hybrid strengthening of short reinforced concrete column elements under eccentric compression. *Structural Concrete, 20*(6), 1955–1973. https://doi.org/10.1002/suco.201800311

Chellapandian, M., Suriya Prakash, S., & Sharma, A. (2017). Strength and ductility of innovative hybrid NSM reinforced and FRP confined short RC columns under axial compression. *Composite Structures, 176*, 205–216. https://doi.org/10.1016/j.compstruct.2017.05.033

Elchalakani, M., & Ma, G. (2017). Tests of glass fibre reinforced polymer rectangular concrete columns subjected to concentric and eccentric axial loading. *Engineering Structures, 151*, 93–104. https://doi.org/10.1016/j.engstruct.2017.08.023

Elchalakani, M., Ma, G., Aslani, F., & Duan, W. (2017). Design of GFRP-reinforced rectangular concrete columns under eccentric axial loading. *Magazine of Concrete Research, 69*(17), 865–877. https://doi.org/10.1680/jmacr.16.00437

El-Emam, H. M., Ata, B., Ahmad, S. S., Salim, H. A., & Reda, R. M. (2024). Enhancing flexural resistance in pre-damaged RC beams with near-surface mounted GFRP bar and bolt anchoring system. *Buildings, 14*(3), 723. https://doi.org/10.3390/buildings14030723

El-Emam, H., El-Sisi, A., Bneni, M., Ahmad, S. S., & Sallam, H. E. D. M. (2020a). Effects of tensile reinforcing steel ratio and Near-Surface-Mounted bar development length on the structural behavior of strengthened RC beams. *Latin American Journal of Solids and Structures, 17*(06), e295.

EL-Emam, H., El-Sisi, A., Reda, R., Bneni, M., & Seleem, M. (2020b). Effect of concrete cover thickness and main reinforcement ratio on flexural behavior of RC beams strengthened by NSM-GFRP bars. *Frattura Ed Integrità Strutturale, 14*(52), 197–210.

El-Sisi, A. A., El-Emam, H. M., El-Kholy, A. E. M. I., Ahmad, S. S., Sallam, H. M., & Salim, H. A. (2022). Structural behavior of RC beams containing unreinforced drilled openings with and without CFRP strengthening. *Polymers, 14*(10), 2034.

Esfandi Sarafraz, M. (2019). Flexural strengthening of RC columns with low longitudinal steel ratio using GFRP bars. *International Journal of Concrete Structures and Materials*. https://doi.org/10.1186/s40069-019-0354-z

Eshaghi-Milasi, S., Mostofinejad, D., Saljoughian, A., & Bahmani, H. (2002). Behavior of RC columns strengthened with UHPFRC jackets through grooving method under eccentric loading: A comparative evaluation of steel and synthetic macro fibers in UHPFRC. *Structural Concrete, 23*(1), 187–206. https://doi.org/10.1002/suco.202100551

Fillmore, B., & Sadeghian, P. (2018). Contribution of longitudinal glass fiber-reinforced polymer bars in concrete cylinders under axial compression. *Canadian Journal of Civil Engineering, 45*(6), 458–468. https://doi.org/10.1016/j.engstruct.2023.115766

Gajdošová, K. B., & Bilčík, J. (2013). Slender rectangular concrete columns strengthened by CFRP confinement and NSMR. *Journal of Composites for Construction, 17*(2), 239–248.

Gao, K., Xie, H., Li, Z., Zhang, J., & Tu, J. (2021). Study on eccentric behavior and serviceability performance of slender rectangular concrete columns reinforced with GFRP bars. *Composite Structures, 263*, 113680. https://doi.org/10.1016/j.compstruct.2021.113680

Hadhood, A., Mohamed, H. M., & Benmokrane, B. (2017). Experimental study of circular high-strength concrete columns reinforced with GFRP bars and spirals under concentric and eccentric loading. *Journal of Composites for Construction*. https://doi.org/10.1061/(asce)cc.1943-5614.0000734

Helal, Y., Garcia, R., Imjai, T., Aosai, P., Guadagnini, M., & Pilakoutas, K. (2024). Seismic behaviour of Exterior RC beam–column joints repaired and strengthened using post-tensioned metal straps. *Bulletin of Earthquake Engineering, 22*, 3261–3286. https://doi.org/10.1007/s10518-024-01904-1

Hussain, Q., Ruangrassamee, A., Jirawattanasomkul, T., & Zhang, D. (2024). Stress and strain relations of RC circular, square and rectangular columns externally wrapped with fiber ropes. *Scientific Reports, 14*(1), 4181. https://doi.org/10.1038/s41598-024-54586-9

Imjai, T., Setkit, M., Figueiredo, F. P., Garcia, R., Sae-Long, W., & Limkatanyu, S. (2022). Experimental and numerical investigation on low-strength RC beams strengthened with side or bottom near surface mounted FRP rods. *Structure and Infrastructure Engineering, 19*(11), 1600–1615. https://doi.org/10.1080/15732479.2022.2045613

Khorramian, K., & Sadeghian, P. (2020). Experimental investigation of short and slender rectangular concrete columns reinforced with GFRP bars under eccentric axial loads. *Journal of Composites for Construction*. https://doi.org/10.1061/(asce)cc.1943-5614.0001088

Khorramian, K., & Sadeghian, P. (2021). Hybrid system of longitudinal CFRP laminates and GFRP wraps for strengthening of existing circular concrete columns. *Engineering Structures*. https://doi.org/10.1016/j.engstruct.2021.112028

Kumutha, R., Vaidyanathan, R., & Palanichamy, M. S. (2007). Behaviour of reinforced concrete rectangular columns strengthened using GFRP. *Cement and Concrete Composites, 29*(8), 609–615. https://doi.org/10.1016/j.cemconcomp.2007.03.009

Mohamed, H. M., Afifi, M. Z., & Benmokrane, B. (2014). Performance evaluation of concrete columns reinforced longitudinally with FRP bars and confined with FRP hoops and spirals under axial load. *Journal of Bridge Engineering*. https://doi.org/10.1061/(asce)be.1943-5592.0000590

Moshiri, N., Hosseini, A., & Mostofinejad, D. (2015). Strengthening of RC columns by longitudinal CFRP sheets: Effect of strengthening technique. *Construction and Building Materials, 79*, 318–325. https://doi.org/10.1016/j.conbuildmat.2015.01.040

Neupane, R. P., Imjai, T., Garcia, R., Chua, Y. S., & Chaudhary, S. (2024). Performance of eccentrically loaded low-strength RC columns confined with posttensioned metal straps: An experimental and numerical investigation. *Structural Concrete*. https://doi.org/10.1002/suco.202301026

Patel, T., Salla, S., Vasanwala, S., & Modhera, C. (2022). Strengthened of a square RC columns using BFRP and GFRP: The experimental investigations. *Trends in Sciences, 19*(15), 5602. https://doi.org/10.48048/tis.2022.5602

Raval, R., & Dave, U. (2013). Behavior of GFRP wrapped RC columns of different shapes. *Procedia Engineering, 51*, 240–249. https://doi.org/10.1016/j.proeng.2013.01.033

Sai Madupu, L. N. K., & Sai Ram, K. S. (2021). Performance of axially loaded reinforced concrete rectangular columns strengthened with GFRP strips. *Materials Today: Proceedings, 43*, 1784–1791. https://doi.org/10.1016/j.matpr.2020.10.454

Sallam, H. E., Badawy, A. A., & El-Emam, H. M. (2013). Numerical simulation of the performance of strengthened RC beams using smeared crack approach. *Journal of Jazan University-Applied Sciences Branch, 2*(2), 30–44.

Samy, K., Fouda, M. A., Fawzy, A., & Elsayed, T. (2022). Enhancing the effectiveness of strengthening RC columns with CFRP sheets. *Case Studies in Construction Materials, 17*, e01588. https://doi.org/10.1016/j.cscm.2022.e01588

Sudhakar, R., & Partheeban, P. (2017). Strengthening of RCC column using glass fibre reinforced polymer (GFRP). *International Journal of Applied Engineering Research, 12*(14), 4478–4483.

Sun, L., Wei, M., & Zhang, N. (2017). Experimental study on the behavior of GFRP reinforced concrete columns under eccentric axial load. *Construction and Building Materials, 152*, 214–225. https://doi.org/10.1016/j.conbuildmat.2017.06.159

Talaeitaba, S. B., Barati, E., & Eslami, A. (2019). Retrofitting of reinforced concrete columns using near-surface-mounted steel rebars and fiber-reinforced polymer straps under eccentric loading. *Advances in Structural Engineering, 23*(4), 687–701. https://doi.org/10.1177/1369433219877793

Triantafyllou, G. G., Rousakis, T. C., & Karabinis, A. I. (2015). Axially loaded reinforced concrete columns with a square section partially confined by light GFRP straps. *Journal of Composites for Construction, 19*(1), 04014035. https://doi.org/10.1061/(ASCE)CC.1943-5614.0000496

Wang, H., Xu, J., Zhao, J., Han, X., Pan, K., Yu, R. C., & Wu, Z. (2024). Axial compression behavior of circular seawater and sea sand concrete columns reinforced with hybrid GFRP-stainless steel bars. *Materials, 17*(8), 1767. https://doi.org/10.3390/ma17081767

Publisher's Note

Seleem S. E. Ahmad Professor at Engineering Materials Department, Zagazig University, Zagazig 44519, Egypt.

Mohamed Yones M.Sc. Student at Engineering Materials Department, Zagazig University, Zagazig 44519, Egypt.

Mahmoud Zaghlal Assistant Professor at Structural Engineering Department, Faculty of Engineering, Zagazig University, Zagazig 44519, Egypt.

Hesham Elemam Assistant Professor at Civil and Environmental Engineering, University of Missouri, Columbia, MO 65211, USA.

Ahmed A. Elakhras Assistant Professor at Engineering Materials Department, Faculty of Engineering, Zagazig University, Zagazig 44519, Egypt.